Acta of Bioengineering and Biomechanics
Vol. 19, No. 3, 2017

Original paper
DOI:10.5277//ABB-00777-2016-02

Investigation of chest injury mechanism caused by different seatbelt loads in frontal impact

SEN XIAO[1, 2], JIKUANG YANG[2, 3]*, JEFF R. CRANDALL[4]

[1] School of Mechanical Engineering, Hebei University of Technology, Tianjin, China.
[2] The State Key Laboratory of Advanced Design & Manufacturing for Vehicle Body, Hunan University, Changsha, China.
[3] Department of Applied Mechanics, Chalmers, University of Technology, Gothenburg, Sweden.
[4] Center for Applied Biomechanics, University of Virginia, Charlottesville, USA.

Purpose: The purpose of this quantitative study is to investigate the differences of the injury mechanism caused by two different types of seatbelt loads on the occupant's chest. *Methods*: The finite element analysis is employed to compare the different responses of the human body model, including comparison of kinematics, chest accelerations, seatbelt forces and chest injury outcomes regarding chest deflections and rib fractures. *Results*: The calculated rib strain–stress response from simulations in force-limiting seatbelt are higher than that in the regular seatbelt. The forward movement and torso twist are both great in simulations with force-limiting seatbelt. Moreover, there are obvious differences in the injury outcomes of chest deflections and rib fracture risks under the different seatbelt loads. *Conclusion*: Results indicate that the chest deflections and rib fracture risks are negatively correlated under the load of the force-limiting seatbelt, However, they are positively correlated to and determined by the seatbelt peak load of the regular seatbelt. This paper can provide a reference for study of the chest injury mechanism and protection efficiency of seatbelt.

Key words: *seatbelt restraint system, human body finite element model, kinematics, rib fractures, chest deflections*

1. Introduction

A recent statistical analysis shows the number of injury cases in traffic accidents is still quite large though the number of fatal injuries has been decreasing dramatically [18]. Among all traffic injuries, the most common cases encountered are chest injuries, especially in frontal impact [19]. About 70% of morbidity injuries are related to chest segment in frontal crash [26] and most of them are related to ribs. Ribs are the primary structure of the thorax and fractures of ribs are the most common and critical chest injury [1]. Chest injuries to the elderly are especially serious and of particular concern [11]. One of the facts is that the ribs of the aged people are more vulnorable than the youngsters because of their mechanical properties [22]. Unfortunately, the study on the chest injuries in accidents for the elderly is not sufficient.

Most chest injuries, especially for the elderly, come from seatbelt loads [4], [29], meanwhile, the influence of large distribution load from safety airbags on the chest injuries is not significant, especially on rib fractures [11]. The seatbelt is the main restraint of occupants in frontal impact. Different seatbelt loads can lead to different kinematic responses and injury outcomes during the impact [28], [29] due to their different functionalities, therefore, they should be thoroughly analyzed.

Most studies about chest injury mechanism are performed by rib bending test [8], [9] or by applying loads to the whole thorax [27]. The influence of the seatbelt restraint system on chest injury is also investigated via simplified sled test [16]. However, there are few reports about the study of chest injuries utilizing a whole scale sled test. Meanwhile, biomechanical experiments can provide important data to verify the finite element (FE) models [3] and finite element

* Corresponding author: Jikuang Yang, The State Key Laboratory of Advanced Design & Manufacturing for Vehicle Body, Hunan University, 410082, Changsha, China. Phone: (+86) 15116210337, e-mail: jikuang.yang@chalmers.se, jikuangyang@hnu.edu.cn
Received: November 5th, 2016
Accepted for publication: June 3rd, 2017

analysis is also a complement to the experiments with detailed physical parameters of strain and stress response. So, simulation study based on biomechanical experiments can be an effective approach to get the more credible results.

There are several chest injury indexes which can represent the chest injuries. Among these, chest deflections and rib fractures caused by the restraint systems are considered the focus of biomechanics study [2]. Chest deflections can reflect the fracture risks of ribs and sternum in frontal crash [12]. Meanwhile, the positions of these fractures can represent the injury of the whole ribcage and injury risks of inner organs [17]. Strain/stress analysis is a useful approach to the injury mechanism. To predict fracture risks with computational method, the rib fracture probabilistic prediction method [5] was utilized based on the post processing of strain besides the usual index like chest deflections and accelerations.

In order to investigate the different chest injury mechanisms caused by seatbelts loads, two simulations are established with a belted human body model (HBM) based on the frontal sled test configuration. The kinematics, chest accelerations, seatbelt forces, 4-point chest deflections and rib fracture risks were analyzed and compared between two simulations of utilizing regular seatbelt and force-limiting seatbelt.

2. Materials and methods

The human body model used in this study is the GHBMC (Global Human Body Models Consortium) version 4.2, which was developed according to the latest biomaterial test and volunteer data. There are total of 2197853 elements and 125933 nodes in this model. The main contact algorithms involved in the model were the automatic surface to surface contact between seatbelt and chest as well as automatic single surface contact among the inner soft tissues.

The chest model included the spine, ribs, costal cartilage, sternum, clavicle, scapula, pelvis and internal organs. The chest was simulated according to the anatomical structure using the material properties from the literature [7]. In the chest of the model, bones were simulated based on elastic-plastic material, and soft tissues were modeled by using superelastic material model. Most of the internal organs were simulated by the combination of shell and solid elements. According to anatomy, a rib consists of the thin cortical bone and internal trabecular bone. The rib cortical bone was simulated with 3 layers of shell elements with the thickness of 0.7–1.2 mm, and hexahedron solid elements for the soft rib cancellous bone. Sharing nodes method was used to connect these two elements. Most of the inner organs (including liquids) and other soft tissues were simulated by solid element except for stomach by airbag. The bio-fidelity of this GHBMC model had been verified on different levels [6]. Particularly, the chest was also confirmed and improved in segment level [13], [14] or the whole body level [20], [21] to have good bio-fidelity. Therefore, this human body model can be used in the following study especially for chest injury mechanism.

Two different seatbelt loads were applied by using two types of seatbelts. The finite element seatbelt was created with material parameters from the manufacturer. The seatbelt was simulated by the combination of 1D beam element and 2D shell element. The shell element was used to simulate the contact between the seatbelt and the body, what provides the load to the chest. Meanwhile 1D beam element was used to connect the seatbelt fix points in sled and belt with shell elements. The loading and unloading curves of the seatbelt were defined in these elements to make the responses of the seatbelt in the simulation the same as the responses in the test. The forces of the 1D beam elements on the upper shoulder, lower shoulder and lap belts were used to represent the seatbelt load on the chest. The loading and unloading curves (Fig. 1) were defined according to the tension test, in which the limiter's setting of force-limiting seatbelt was 2.7 kN. Contact friction coefficient 0.4 was selected in the contact between the chest and belt.

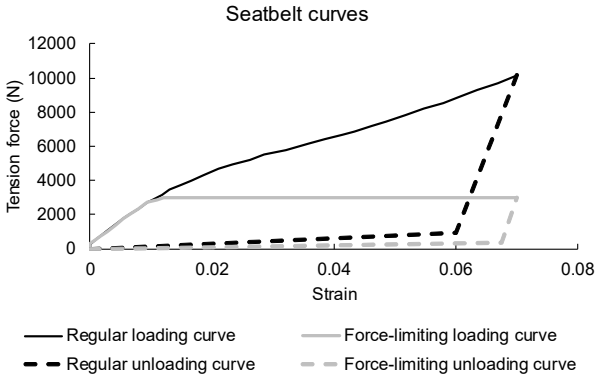

Fig. 1. The loading and unloading curves of regular (dark) and force-limiting (grey) seatbelts

The simulation was established according to the same boundary conditions as these of sled test (Fig. 2) which was named the Gold Standard (GS) test [25]. This sled was built according to the widely used middle size vehicle in the USA. The deceleration pulse applied on the sled was corresponding to the impact

speed of 40 km/h, which was the speed also found in the crashes statistics for serious chest injuries with seatbelt restraint occupant. The coordinate system located at the sled was defined as follows. The forward direction was defined as the positive X-direction and the downward direction as positive Z-direction. The kinematics measuring points were recorded by motion capture system, and these points were the head, the first thoracic vertebra (T1), the eighth thoracic vertebra (T8), the second lumbar vertebra (L2), the fourth lumbar vertebra (L4), the pelvis and two shoulders (Lsh and Rsh). The bio-fidelity of this established whole model had been validated via the comparison of kinematics, forces and deflections [30].

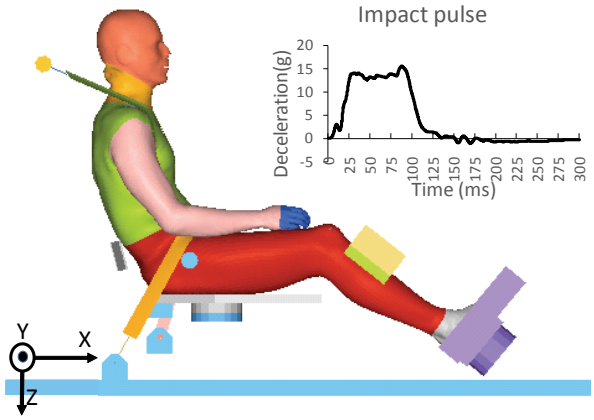

Fig. 2. The belted occupant model and impact pulse

Four-point chest deflections were defined according to the measuring devices in THOR (Test Device for Human Occupant Restraint) dummy [24]. These measuring results can reflect the independent deflection at four locations of the chest. They were located at 40 mm from the sternum vertical centerline in the rib 4 and at 80 mm from the sternum vertical centerline in the rib 8. These deflections were more informative than the maximum chest deflection which was generally used in former dummy test. Strain–stress analysis was adopted to study the tolerance and predict chest injury risks. In particular, rib fractures were determined by the ultimate strain/stress. The distribution of the strain/stress can reflect the locations of fractures and the change of fracture risks. The rib fracture risk prediction method was based on the post process of strain analysis [5]. Age and injury level were also taken into account when calculating the fracture risks.

The simulation matrix (Table 1) was built to analyze the differences of chest injury mechanism caused by different seatbelt loads. Two simulations were conducted with LS-DYNA MPP.

Table 1. Simulation matrix

Simulation	Seatbelt loads
S 1	Load of regular seatbelt
S 2	Load of force-limiting seatbelt

3. Results

3.1. Kinematics

The entire impact process lasted for around 175 ms and the biggest difference between the two simulations happened from 90 ms to 120 ms. Thus, the com-

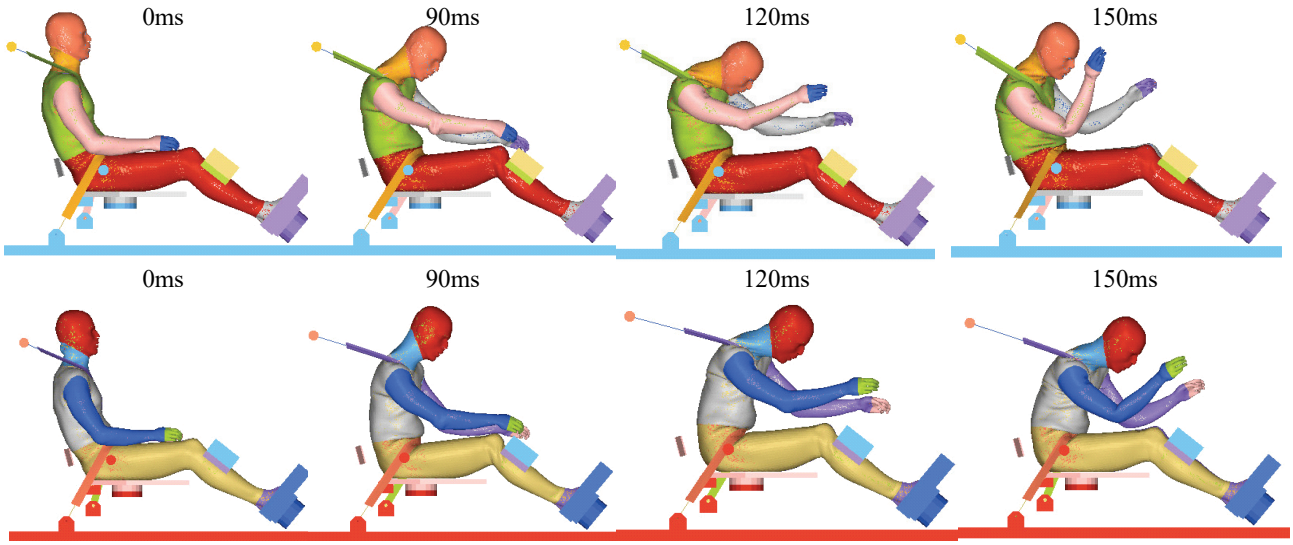

Fig. 3. Comparison of kinematic process (first row: regular seatbelt, second row: force-limiting seatbelt)

parison figures (Fig. 3) selected were at 0 ms, 90 ms, 120 ms and 150 ms.

Comparison of the kinematic process demonstrated that the human body in force-limiting seatbelt would move forward and further and twist less. Meanwhile, the rotation movement of head and two shoulders was little and the change of the chest shape was small. Moreover, force-limiting seatbelt can significantly reduce the torso rotation. A big difference was found at 120 ms when the human body still went forward in simulation of force-limiting seatbelt. Meanwhile, the body reached the furthest position and went backward in the regular seatbelt simulation.

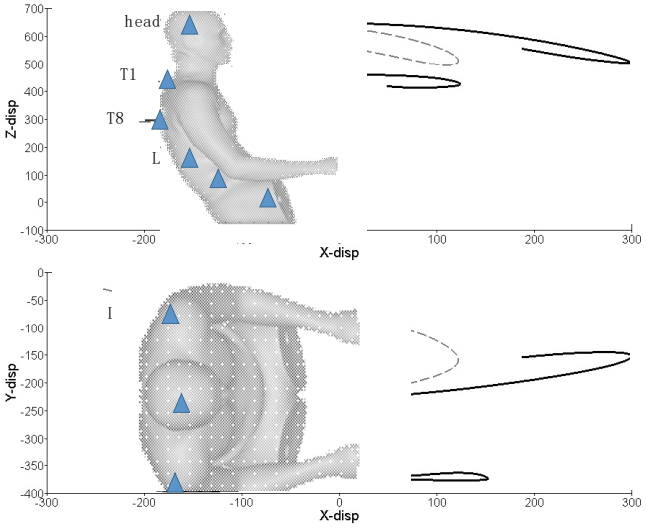

Fig. 4. Comparison of kinematic trace in measuring points (solid line: force-limiting seatbelt, dash line: regular seatbelt)

The kinematics traces (Fig. 4) can clarify the results of the kinematic process. The body displacement in the X-direction was larger in the force-limiting seatbelt, and the contact process duration lasted for 175 ms which was longer than the contact duration of regular seatbelt. The decline in Z-direction was about 6 mm to 13 mm smaller than the regular one. The difference in the kinematics mainly appeared in head and the upper torso (head, T1, T8, L2), and the greatest one occurred in T1 with 180 mm. The torso rotation in the regular seatbelt was larger than the rotation in force-limiting one. When the peak of forward displacement occurred, the rotation difference was 16 mm in head as well as 28 mm and 56 mm for the two shoulders between the two seatbelt loads. The body rotation in the simulation of force-limiting seatbelt simulation was quite small, especially in the two shoulders. In contrast, the body rotation in the simulation of regular seatbelt was more noticeable.

3.2. Chest accelerations

Chest acceleration can reflect the change rate of speed which is an indicator of inner organ injury. All the acceleration curves were processed using SAE filter at 60 Hz. The comparison of chest accelerations (Fig. 5) between the two simulations showed that the function of force-limiting seatbelt would last longer (about 40–50 ms) in holding the human body position. Chest acceleration curves in both simulations were nearly the same for the first 48 ms. Then, differences occurred after they both reached the peak accelerations at about 50 ms. The peak chest accelerations were 23.76 g at 52 ms for regular seatbelt, and 16.82 g at 52 ms for force-limiting seatbelt.

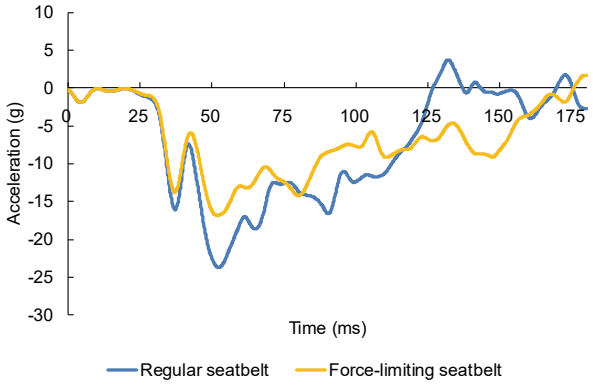

Fig. 5. Comparison of chest accelerations

Chest accelerations in both simulations started becoming distinctive after 25 ms, and the first peak appeared at 37.5 ms. After that, the acceleration in regular seatbelt simulation would rise again until reach the second and biggest peak. Then the curve dropped to the acceleration 0 g at 125 ms. In a comparison, several similar amplitude peaks appeared during the period 50–80 ms in force-limiting seatbelt. Then, the curve decreased slowly to acceleration 0 g at around 175 ms.

3.3. Seatbelt tension force

The seatbelt forces were measured at three locations (the upper shoulder belt, the lower shoulder belt and the right lap belt) to identify the loads in different parts of the seatbelt. The difference of seatbelt force can directly reflect the functionality of seatbelt force limiter (Fig. 6).

It can be observed that once the load of force-limiting seatbelt went up to 2.7 kN, the force value remained constant (at 2.7 kN) until the torso began to move backwards. However, the function time was longer. The force would change with the torso move-

ment position and the seatbelt function also lasted longer in force-limiting seatbelt. As a comparison, regular seatbelt force would increase until the torso reached the far forward position. However, regular seatbelt directly held the whole torso with slight elongation, and functioned for this kind of seatbelt would last for a shorter time.

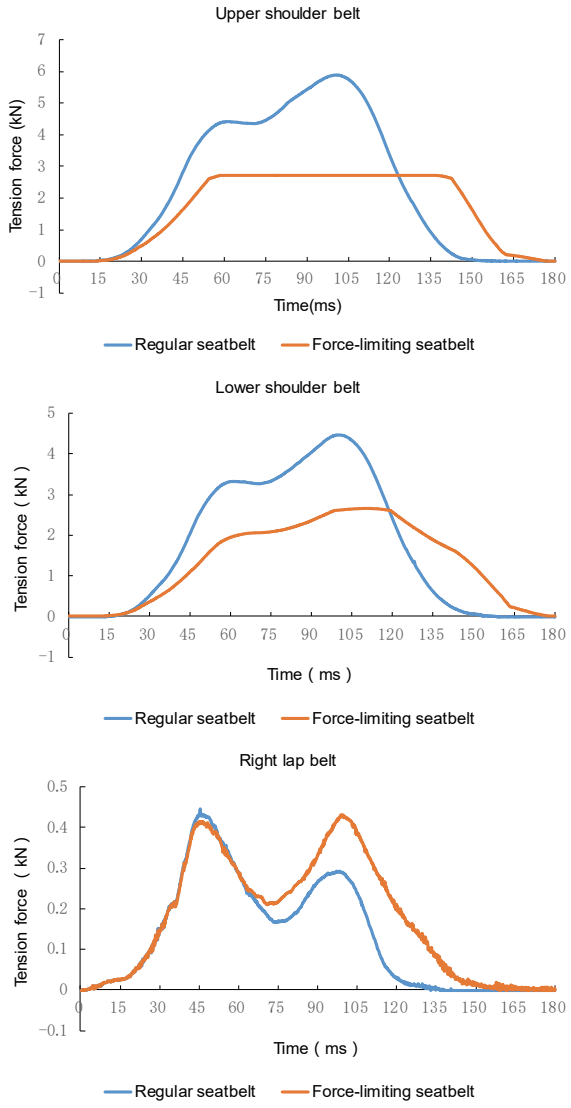

Fig. 6. Comparison of the seatbelt tension forces

If closely inspected, some noticeable differences can be observed between the two simulations in seatbelt forces. The periods of the regular seatbelt function force were 15 ms to 25 ms less than the force-limiting ones in three seatbelt tension measuring positions. The peak force of lower regular shoulder belt was also higher than the force of force-limiting belt. The force change was the same as the upper shoulder belt without a smooth period. The force and process of the lap belt in the two kinds of seatbelts were nearly the same, although the force in regular seatbelt in the later period of this comparison was lower. There were two stages in the regular seatbelt because the chest was a stiffness variable rate system, while for the force-limiting seatbelt, there was no obvious change of the slop in the force curves. The differences between these forces of two seatbelts were 3.19 kN in upper shoulder belt, 1.81 kN in lower shoulder belt and 0.02 kN in right lap belt.

3.4. Chest deflection

The processes of 4-point chest deflections were compared (Fig. 7). The chest deflection measuring locations were the upper right (UR), the upper left (UL), the lower right (LR) and the lower left (LL). The results indicated that the deflections had the same tendencies in both simulations though the particular values varied.

The changing of the deflection process between the simulations with two different seatbelts were almost identical. Chest deflections in UR, UL and LL were all compression, and the deflection in LR went in the opposite direction of other three measuring points. All deflections showed significant differences between two seatbelt simulations, which indicated the loads of the two seatbelts were different. The biggest difference happened in the LL regarding force-limiting seatbelt, which meant the compression at this measuring point became less and far less than the extension compared with regular seatbelt. Although the duration time of the force-limiting was longer than that of the regular seatbelt (except LR), the peaks in both simulations occurred nearly at the same time. Deflection processes of LR in both simulations were nearly the same especially for the first peak. This LR point was also the farthest measuring point from the seatbelt. These results may illustrate that the influence of the seatbelt parameters on the deflection of this point was very small. The significant compression time of measuring points UR and UL were 40 ms later than the time of regular seatbelt. While the LL would go extension at 25 ms then compress at 75 ms in force-limiting seatbelt, the LL deflection would keep compressing from 50 ms until the end of regular seatbelt simulation.

Comparing the chest peak deflections in the two simulations, all the deflections in force-limiting seatbelt were lesser than the ones in regular seatbelt. The extensions were also large, which meant the safety space for inner organs would become larger. The biggest difference of 20 mm was found in LL measuring point. The differences at the upper torso measuring points were no less than 10 mm.

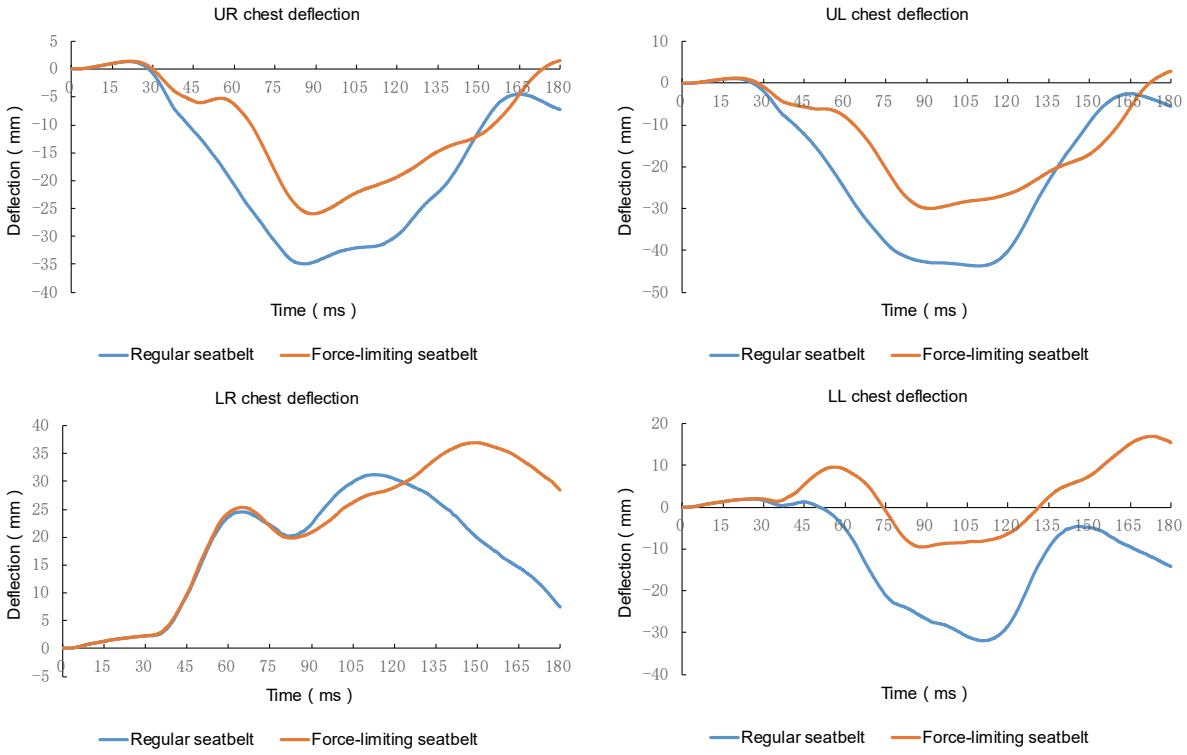

Fig. 7. Comparison of 4-point chest deflections ("–": compression, "+": extension)

2.5. Strain and stress analysis

The strain and stress were usually used to determine the chest injury mechanism. The reference strains of 0.018 [9], 0.027 [15] and stresses of 124.3 MPa [15], 143.4 MPa [23] were used in the legend of the contour plots. These values were obtained to define the fracture tolerance. Strain and stress distribution plots can illustrate the injury locations and injury possibilities. Judging from the strain/stress plots, the rib 6 to rib 10 had a high tendency to fracture, which was also noted in the sled test [25]. Most of the peak strains –stresses of each rib happened in the period from 100 ms to 130 ms.

The strains of the regular seatbelt simulation were widely distributed over the areas of peak value (Fig. 8) and these distribution areas were similar to those in the force-limiting seatbelt. There were significant differences of strain among rib 5, rib 7, rib 8 in left and rib 4 in right, in which there were more high strain spots in the lateral ribcage. The strain distribution areas in rib 1 on both sides of the two simulations were also different in which the high strain area was larger than in the case of the force-limiting one. Though the values were nearly in the same level for other ribs, there were nearly no high strain area in upper ribcage. The changes of peak strains and high strain areas from 100 ms to 130 ms, were small in both simulations.

Regarding the ribcage stress distribution (Fig. 9), the peak value was found in the force-limiting seatbelt simulation. Most of the high stress areas were located near the joint between rib and costal cartilage especially in the rib 1 and rib 6 to rib 9. There were more than one peak stress spots or areas of each rib in the simulation of regular seatbelt, especially the rib 7 and rib 8 in left. There was a large high stress area in the right ribcage in force-limiting seatbelt simulation, especially from rib 6 to rib 8. High stress areas were also found in rib 1 and rib 6 to rib 8 on two sides in both simulations. The high stress area occurred in regular seatbelt changed a little more than the force-limiting one, especially in left lateral ribcage. Meanwhile, the peak stresses did not change much.

3.6. Fracture risks

First principle strain was utilized in the probabilistic method in the chest injury prediction. For clarity, the rib fracture risks were divided into four groups: lower than 25%, 25 to 50%, 50 to 75% and higher than 75%, which represented the low, middle, serious and high injury risk of fracture, respectively. The age used in this study was 55-year-old,

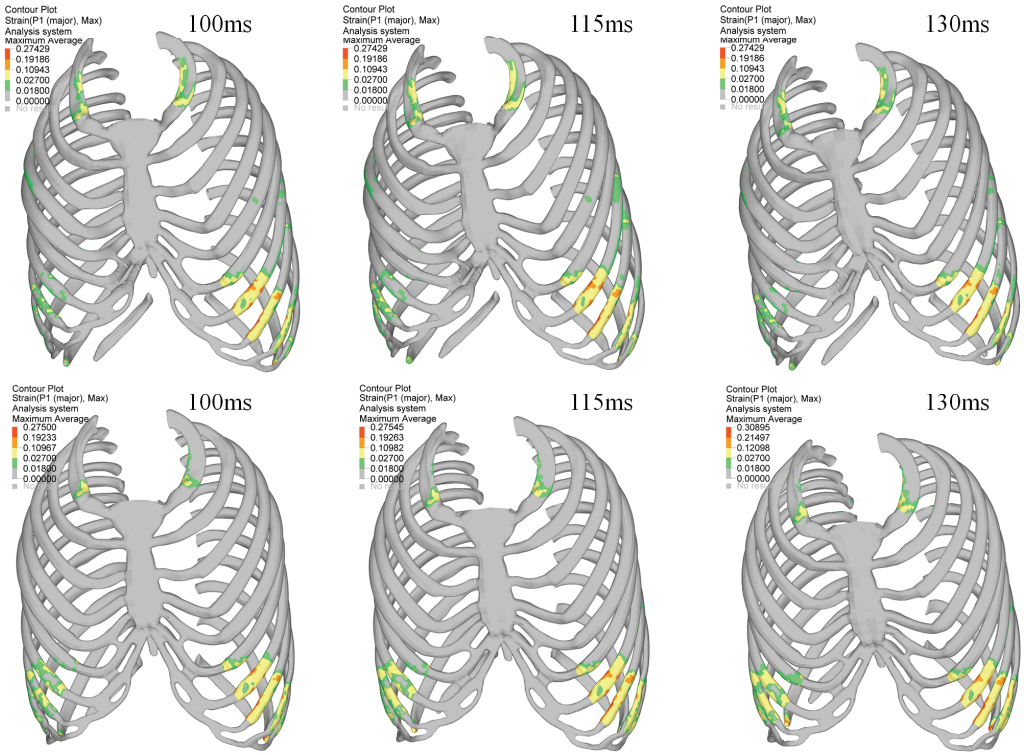

Fig. 8. Strain distribution of the ribcage (first row: regular seatbelt, second row: force-limiting seatbelt)

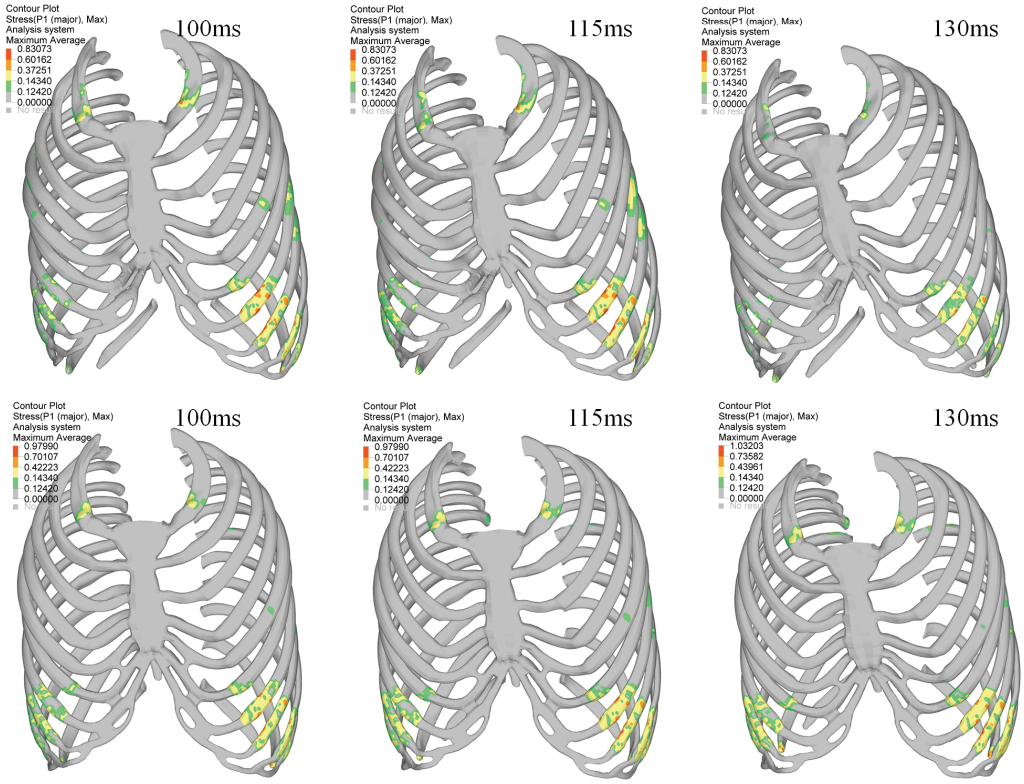

Fig. 9. Stress distribution of the ribcage (first row: regular seatbelt, second row: force-limiting seatbelt)

which represented the average age of the subjects in the sled tests.

Most of the fracture risks were found in the force-limiting seatbelt simulation (Fig. 10). Specifically, the risks of rib 1 and rib 6 to rib 11 on both sides were close to 100%. Meanwhile, high injury risks mostly happened in left rib 7 to rib 9 and rib 11 in regular seatbelt simulation. Besides, the fracture risks of other ribs

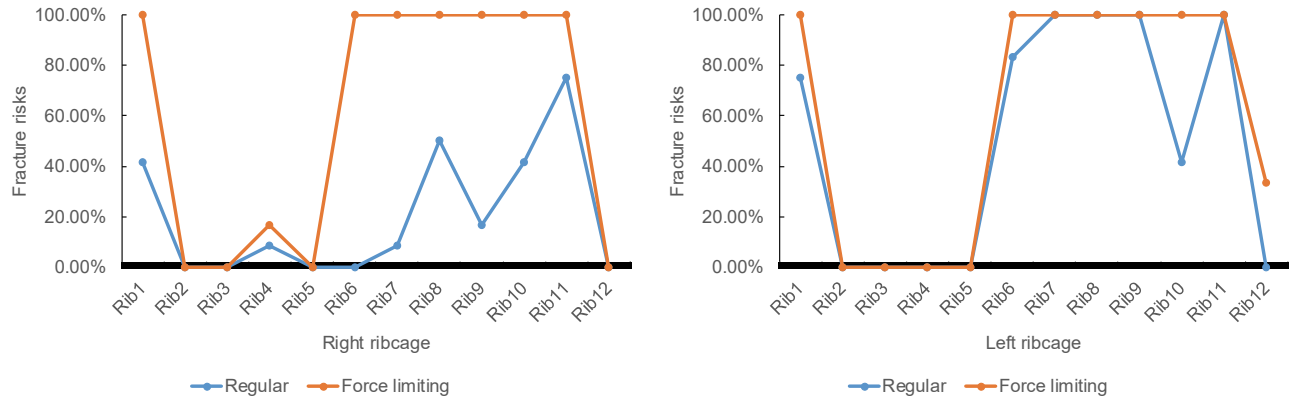

Fig. 10. Comparison of ribcage injury risks (@55-year-old)

Table 3. Comparison of ribcage injury risks in different seatbelt simulations (@55-year-old)

Simulation ID	The prediction risks of n+ fractured ribs								
	1+	2+	3+	4+	5+	6+	7+	8+	9+
S 1	100.00%	100.00%	100.00%	100.00%	99.93%	98.88%	92.89%	75.52%	47.32%
S 2	100.00%	100.00%	100.00%	100.00%	100.00%	100.00%	100.00%	100.00%	100.00%

were smaller in regular seatbelt than those in force-limiting simulation, especially for ribs in the right ribcage. The risk differences between the two simulations of rib 6 to rib 11 on the right side were about 50%, in while the predicted risks of rib 2 to rib 5 on both sides and rib 12 on both sides were small in both simulations, which meant no fracture would occur in these ribs. The results of rib fracture risks from the two simulations in rib 1 and rib 6 to rib 10 were large because of the different kinematic results and seatbelt function times. The differences of rib fracture that happened in the simulations were attributed to the torso twist regarding the seatbelt path. In this study, the left ribcage was more sensitive to the deflection and rib fracture risks. Peak deflections in left ribcage were much larger than those in right.

The fracture risks of the whole ribcage would change with the increase of the number of fractured ribs (Tab. 3). When the number of fractured ribs was less than 4+, the injury risk would always be 100% in both seatbelt simulation results though the number of fractured ribs rose. When the number of fractured ribs was greater than 5+, the injury risks would decrease accordingly in regular seatbelt simulation with the increase of number of fractured ribs. As for 7+ fractured ribs, the risks would decline from 92.89% (7+) to 47.32% (9+), meanwhile, injury risks were always closed to 100% if the number of fractured ribs was no less than 9+ in force-limiting seatbelt simulation. This indicated there would be at least 10 fractured ribs in the ribcage in the simulation of force-limiting seatbelt. Most of the fracture risks were more than 90%, which were very serious.

4. Discussion

Different seatbelt loads will have unique influence on the chest injuries. Seatbelt should prevent the excessive chest deflection as well as reduce the injury risk during the impact. As far as the force-limiting seatbelt, in concerned the chest compression is small and the injury risk is high. In this case, airbags should be used with force-limiting seatbelt to limit rib fracture risks by reducing forward movement. However, the chest deflection is large and the injury risk is small for regular seatbelt. Therefore, the regular seatbelt alone can well protect the ribcage (ribs) though the injury is still serious. Meanwhile, the chest deflection may reflect that other chest injuries are also serious. This can explain the fact that the airbag and force-limiting seatbelt are common equipment in the frontal row, while the back row usually equipped with the regular seatbelt.

Two sets of chest injury outcomes exhibit different trends in the two seatbelt-load simulations. The correlation between the two injury indicators, chest deflection and injury risk is inconsistent in the

force-limiting seatbelt model, such as the chest deflection is large, while the injury risk is high, and the correlation between these indicators of regular seatbelt simulation is consistent, in which the rib fracture risk is high when the chest deflection is large.

According to the study of Shaw [25], there are no obvious fractures found in the ribcage when the force-limiting seatbelt test is performed under the speed of 30 km/h. But in the current study, chest injury is serious at 40 km/h. This indicates there is a specific speed between 30 km/h and 40 km/h, which is the speed for airbags to get function. If the impact speed is greater than this specific speed, only the regular seatbelt or the force-limiting seatbelt combined with airbags will provide a good protection of chest from frontal impact. If the impact speed is smaller than this specific speed, the force-limiting seatbelt alone will perform well in the protection. The regular seatbelt can be used isolated at the speed of 40 km/h or 30 km/h. Meanwhile, the force-limiting seatbelt can be used alone at a speed of 20 km/h or with other equipment when used under a speed of 40 km/h.

In this study regarding the bio-fidelity validation with the sled test, the tensioner of seatbelt which may affect the seatbelt loads is not included. However, the belt pretensioner is now widely used in cars to reset slack on the belt and to attract the passenger to seat during the accident. This solution has also been very important for the obtained values of forces and displacements on the chest. Therefore the influence of belt pretensioner should be conducted in the future.

Seatbelt load can affect the chest injury outcomes. The seatbelt will elongate, though the load will remain at a certain level when the tension force reaches the setting of force limiter in the force-limiting seatbelt. So, the chest deflections are less. But the regular seatbelt has a very huge peak force which will cause serious deflection. This indicates the peak seatbelt force and the seatbelt elongation will affect the final chest deflection.

This study is conducted based on the sled tests with restraint of seatbelt only. This means when the impact speed is higher than 40 km/h, the load strength would be too high to analyze the injury mechanisms regarding rib fractures for the test subjects. Besides, the impact speeds like more than 80 km/h are seldom studied because of the fatal boundary conditions to the occupant even equipped with the ordinary safety equipment like seatbelts and airbags. Therefore, right now the simulations at the impact speeds of more than 40 km/h are not conducted in this study.

5. Conclusions

The difference of chest injury mechanism caused by two different seatbelt loads was investigated by means of frontal sled test simulation with a human body model. Then, the injury mechanism was analyzed with respect to the kinematics and dynamics from two simulations. The results can provide a better understanding of the chest injury mechanism and the study method can serve as a reference to the improvement of the seatbelt protection efficiency.

The results show that deflections and rib fracture risks are negatively correlated for the force-limiting seatbelt, which is determined by the forward displacement and seatbelt load duration. However, they are positively correlated to and determined by the seatbelt peak load for the regular seatbelt. Furthermore, there is a difference in the chest injury outcomes between the two chest loads due to the seatbelt unique function.

Acknowledgement

This work was supported by funds from China Scholarship Council (CSC). Jing Huang, Fuhao Mo, Zhi Xiao and Bingbing Nie take part in the discussion of this study. The authors would like to acknowledge their contribution to this study.

References

[1] BAKER S.P., O'NEILL B., HADDON JR W., LONG W.B., *The Injury Severity Score: A Method for Describing Patients with Multiple Injuries and Evaluating Emergency Care*, Journal of Trauma and Acute Care Surgery, 1974, 14(3), 187–196.

[2] BOSTROM O., HALAND Y., BOSTROM O., HANLAND Y., *Benefits of a 3+2-Point Belt System and an Inboard Torso Side Support in Frontal, Far-Side and Rollover Crashe*s, International Journal of Vehicle Safety, 2005, 1(1/2/3).

[3] CRANDALL J.R., BOSE D., FORMAN J., UNTAROIU C.D., ARREGUI-DALMASES C., SHAW G., *Human Surrogates for Injury Biomechanics Research*, Clinical Anatomy, 2011, 24, 362–371.

[4] EVANS L., *Airbag Effectiveness in Preventing Fatalities Predicted According to Type of Crash, Driver Age, and Blood Alcohol Concentration*, 33rd Annual Proceedings of the Association for the Advancement of Automotive Medicine, Des Plaines, IL, 1989.

[5] FORMAN J.L., KENT R.W., MROZ K., PIPKORN B., BOSTROM O., SEGUI-GOMEZ M., *Predicting Rib Fracture Risk with Whole-Body Finite Element Models: Development and Preliminary Evaluation of a Probabilistic Analytical Framework*, Annals of Advances in Automotive Medicine, 2012, 56, 109–124.

[6] GAYZIK F.S., MORENO D.P., VAVALLE N.A., RHYNE A.C., STITZEL J.D., *Development of the Global Human Body Models Consortium Mid-Sized Male Full Body Model,* International Workshop on Human Subjects for Biomechanical Research, 39, National Highway Traffic Safety Administration, US DOT, 2011.

[7] GHBMC LLc, *GHBMC_M50-O_v4-2_Manual*, 2014.

[8] KEMPER A.R., MCNALLY C., KENNEDY E.A., MANOOGIAN S.J., RATH A.L., NG T.P., STITZEL J.D., SMITH E.P., DUMA S.M., MATSUOKA F., *Material Properties of Human Rib Cortical Bone from Dynamic Tension Coupon Testing*, Stapp Car Crash J., 2005, 49, 199–230.

[9] KEMPER A.R., MCNALLY C., PULLINS C.A., FREEMAN L.J., DUMA S.M., ROUHANA S.M., *The Biomechanics of Human Ribs: Material and Structural Properties from Dynamic Tension and Bending Tests*, Stapp Car Crash J., 2007, 51, 235–273.

[10] KENT R., LESSLEY D., SHERWOOD C., *Thoracic Response Corridors for Diagonal Belt, Distributed, Four-Point Belt, and Hub Load*, Stapp Car Crash Journal, 2004, 48, 495–519.

[11] KENT R., PATRIE J., *Chest Deflection Tolerance to Blunt Anterior Load Is Sensitive to Age but Not Load Distribution*, Forensic Science International, 2005, 149(s 2–3), 121–128.

[12] KENT R.W., SHERWOOD C.P., LESSLEY D.J., OVERBY B., MATSUOKA F., *Age-related Changes in the Effective Stiffness of the Human Thorax Using Four Load Conditions*, IRCOBI Conference on the Biomechanics of Impact, 2003.

[13] LI Z., KINDIG M.W., KERRIGAN J.R., UNTAROIU C.D., SUBIT D., CRANDALL J.R., KENT R.W., *Rib Fractures Under Anterior-Posterior Dynamic Loads: Experimental and Finite Element Study*, Journal of Biomechanics, 2010, 43, 228–234.

[14] LI Z., KINDIG M.W., SUBIT D., KENT R.W., *Influence of Mesh Density, Cortical Thickness and Material Properties on Human Rib Fracture Prediction*, Medical Engineering & Physics, 2010, 32, 998–1008.

[15] MORDAKA J., MEIJER R., ROOIJ L.V., ZMIJEWSKA A., *Validation of a finite Element Human Model for Prediction of Rib Fractures*, Proceedings of SAE World Congress & Exhibition Detroit, US: SAE, 2007, Paper 200701-1161.

[16] MURAKAMI D., KOBAYASHI S., TORIGAKI T., KENT R., *Finite Element Analysis of Hard and Soft Tissue Contributions to Thoracic Response: Sensitivity Analysis of Fluctuations in Boundary Conditions*, Stapp Car Crash Journal, 2006, 50(2006-22-0008), 169–189.

[17] NAHUM A.M., MELVIN J.W., *Accidental Injury: Biomechanics and Prevention*, 2nd Edition, Springer-Veriag Inc., New York 2002.

[18] National Bureau of Statistics of the People's Republic of China, Statistical Communiqué of the People's Republic of China on the 2015 National Economic and Social Development, 2016, http://www.gov.cn/xinwen/2016-02/29/content_5047274.htm, Accessed: 30 June 2016.

[19] NIRULA R., PINTAR F.A., *Identification of Vehicle Components Associated with Severe Thoracic Injury in Motor Vehicle Crashes: A CIREN and NASS Analysis*, Accident Analysis and Prevention, 2008, 40(1), 137–141.

[20] PARK G., KIM T., CRANDALL J.R., ARREGUI-DALMASES C., LUZON-NARRO J., *Comparison of Kinematics of GHBMC to PMHS on the Side Impact Condition*, 2013 IRCOBI Conference, Gothenburg, 2013.

[21] PARK G., KIM T., PANZER M.B., CRANDALL J.R., *Validation of Shoulder Response of Human Body Finite-Element Model (GHBMC) Under Whole Body Lateral Impact Condition*, Annals of Biomedical Engineering, 2016, 1–19.

[22] PEZOWICZ C., GŁOWACKI M., *The Mechanical Properties of Human Ribs in Young Adult*, Acta Bioeng. Biomech., 2012, 14(2), 53–60.

[23] PLANK G.R., KLEINBERGER M., EPPINGER R.H., *Analytical Investigation of Driver Thoracic Response to Out of Position Airbag Deployment*, Stapp Car Crash J., 1998, 42, 317–329.

[24] RANGARAJAN N., FOURNIER E., DALMOTAS D., RHULE D., PRITZ H., EPPINGER R., HAFFNER M.P., FULLERTON J., BEACH D., SHAMS T., WHITE R., *Design and Performance of the THOR Advanced Frontal Crash Test Dummy Thorax and Abdomen Assemblies*, International Technical Conference on the Enhanced Safety of Vehicles (ESV), 1998, 16.

[25] SHAW C.G., PARENT D.P., PURTSEZOV S., LESSLEY D., CRANDALL J., KENT R., GUILLEMOT H., RIDELLA S.A., TAKHOUNTS E., MARTIN P., *Impact Response of Restrained PMHS in Frontal Sled Tests: Skeletal Deformation Patterns Under Shoulder Seatbelt Load*, Stapp Car Crash J., 2009, 53(2009-22-0001), 1–48.

[26] SHIN J., UNTAROIU C., LESSLEY D., CRANDALL J., *Thoracic Response to Shoulder Belt Load: Investigation of Chest Stiffness and Longitudinal Strain Pattern of Ribs*, SAE, 2009, Technical Paper 2009-01-0384, DOI: 10.4271/2009-01-0384.

[27] WANG F., YANG J.K., MILLER K., LI G., JOLDES G.R., DOYLE B., WITTEK A., *Numerical Investigations of Rib Fracture Failure Models in Different Dynamic Load Conditions*, Computer Methods in Biomechanics and Biomedical Engineering, 2016, 19(5), 527–537.

[28] XIAO S., FORMAN J., YANG J., PANZER M., NIE B., XIAO Z., CRANDALL J., *A Study of the Influence between Regular and Force-limiting Seatbelt on Chest Outcome with Human Body Model in Frontal Impact Tests*, 2015 The International Forum of Automotive Traffic Safety, Xiamen, China, 2015.

[29] XIAO S., YANG J., FORMAN J., PANZER M., XIAO Z., CRANDALL J., *Effect of Contact Friction between Seatbelt and Human Body Model on Simulation of Rib Fracture in Frontal Impact*, Eighth International Conference on Measuring Technology and Mechatronics Automation., 2016, 255–257.

[30] XIAO S., YANG J.K., XIAO Z., CRANDALL J.R., *Analysis of Chest Injury in Frontal Impact via Finite Element Modelling Based on Biomechanical Experiment*. Chinese Journal of Theoretical and Applied Mechanics. 2017, 49(1).

[31] ZHOU Q., ROUHANA S., MELVIN J., *Age Effects on Thoracic Injury Tolerance, Society of Automotive Engineers*, Warrendale, PA, 1996, Paper 962421.